JOURNAL OF COMPUTATIONAL PHYSICS 113, 5–12 (1994)

The Boundary Forced MKdV Equation

L. R. T. GARDNER, G. A. GARDNER, AND T. GEYIKLI

School of Mathematics, University of Wales, Bangor, Gwynedd LL57 1UT, United Kingdom

Received May 12, 1993; revised October 26, 1993

An unconditionally stable numerical algorithm for the modified Korteweg–de Vries equation based on the B-spline finite element method is described. The algorithm is validated through a single soliton simulation. In further numerical experiments forced boundary conditions $u = U_0$ are applied at the end $x = 0$ and the generated states of solitary waves are studied. By long impulse experiments these are shown to be generated periodically with period ΔT_B proportional to U_0^{-3} and to have a limiting amplitude proportional to U_0. This limit is achieved by all waves, after the first, provided the experiment proceeds long enough. The temporal development of the derivatives $U'(0, t)$, $U''(0, t)$ and $U'''(0, t)$ is also periodic, with period ΔT_B. The effect of negative forcing is to generate a train of negative waves. The solitary wave states generated by applying a positive impulse followed immediately by an negative impulse, of equal amplitude and duration, is dependent on the period of forcing. The solitary waves generated by these various forcing functions possess many of the attributes of free solitons.

1. INTRODUCTION

The modified Korteweg–de Vries (MKdV) equation plays a significant rôle in the study of non-linear dispersive waves. It has been found to describe a wide class of physical phenomena such as acoustic waves in anharmonic lattices [1] and Alfén waves in collisionless plasmas [2].

Analytical studies of the MKdV equation have been given by several authors [1–3]. When the normalised MKdV equation

$$u_t + \varepsilon u^2 u_x + \mu u_{xxx} = 0, \tag{1}$$

where the subscripts t and x denote differentiation and ε and μ are positive constants, is solved analytically in an unbounded region with the physical boundary conditions $u \to 0$ as $x \to \pm\infty$ it has a solution of the form [1]

$$\begin{aligned} u(x, t) &= kp \operatorname{sech}(kx - kx_0 - k^3\mu t), \\ p &= \sqrt{6\mu/\varepsilon}, \end{aligned} \tag{2}$$

which represents a single soliton originally sited at x_0 moving to the right with velocity $k^2\mu$. Such solitons may have positive or negative amplitudes depending on the sign of k, but all have positive velocities. It is expected that this analytic solution will also be valid for bounded regions which are sufficiently large.

The exact two-soliton solution, under the conditions given above, is [4]

$$u(x, t) = ip(\log[f^*/f])_x,$$

where * denotes the complex conjugate and

$$\begin{aligned} f &= 1 + i\exp(\eta_1) + i\exp(\eta_2) - \beta\exp(\eta_1 + \eta_2), \\ \eta_j &= k_j x - k_j^3 \mu t + \eta_j^0, \qquad \text{where} \quad j = 1, 2, \\ \beta &= \left(\frac{k_1 - k_2}{k_1 + k_2}\right)^2. \end{aligned}$$

This represents two solitons of amplitudes $k_j p$ and velocities $k_j^2\mu$. When the soliton with the larger amplitude is originally sited on the left, a collision eventually occurs during which each wave undergoes a phase shift of magnitude

$$\begin{aligned} \vartheta &= \Delta/k_j, \\ \Delta &= \log(1/\beta), \end{aligned} \tag{3}$$

that of the larger being positive and that of the smaller being negative.

Solutions of the MKdV equation subjected to the above boundary conditions obey an infinity of conservation laws of which the lowest four invariants are [3]

$$\begin{aligned} I_1 &= \int_{-\infty}^{\infty} u\,dx, \\ I_2 &= \int_{-\infty}^{\infty} u^2\,dx, \\ I_3 &= \int_{-\infty}^{\infty} \left(u^4 - \frac{6\mu}{\varepsilon} u_x^2\right) dx, \\ I_4 &= \int_{-\infty}^{\infty} \left(u^6 - \frac{30\mu}{\varepsilon} u^2 u_x^2 + \frac{18\mu^2}{\varepsilon^2} u_{xx}^2\right) dx. \end{aligned} \tag{4}$$

0021-9991/94 $6.00

The physical boundary conditions usually appropriate for the Korteweg–de Vries (KdV) and the regularised long wave (RLW) equations are $u \to 0$ as $x \to \pm\infty$. However, when these eqations are solved over a semi-infinite region $0 \leqslant x < \infty$ with a non-homogeneous boundary condition $u = u_0$, a constant, at $x = 0$, a source of solitary waves develops at the point $x = 0$ [5–7] and boundary forcing is said to occur. In this paper the effects of such a boundary condition on solutions of the MKdV equation are studied through computer simulation.

Numerical solutions using pseudospectral methods, split-step Fourier methods, and B-spline finite element methods have been given [3, 4, 8]. We have previously used the B-spline finite element method in the study of solitons and solitary waves of the KdV and other non-linear wave equations [8–10].

The B-spline finite element method differs from the usual finite element formulation in that the parameters of the trial function are not the nodal values of the variable u and its derivatives but are the coefficients δ_j of the B-splines which form the local element trial functions. The nodal values are related to δ_j through simple linear relationships and so they are easily obtained when required. An important advantage of this approach is that the δ_j are all of the same type, whereas in the conventional approach function values and derivatives which may be of very different orders of magnitude are mixed together in the nodal vector. A second advantage is that B-spline finite elements have higher order continuity than Hermite elements of similar order. Recently the B-spline finite element method has been extended to a non-uniform mesh [11]. Work is in hand to extend its application also to two dimensions.

The Galerkin approach with cubic B-spline finite elements used for the numerical solution of the quadratically non-linear RLW [9] and KdV [12] equations leads to accurate, unconditionally stable algorithms with, however, rather high operation counts, as shown in Table I, where N_{el} is the number of elements and N_{it} the number of iterations per timestep. If the same approach is used for the cubically non-linear MKdV equation the operation count is increased significantly; by a factor ~ 7 per time step, principally for the determination of the non-linear term.

A collocation method with quintic B-spline finite elements has also been used for the numerical solution of the KdV equation [10]. This results in a considerable reduction in the operation count; see Table VII. In fact, this collocation approach produces a faster, unconditionally stable, algorithm which is easy to implement and has a L_2 error norm for a single soliton simulation comparable in magnitude to that of the above Galerkin formulations. With a collocation approach to the numerical solution of the MKdV equation using quartic B-spline elements a set of $N_{el} + 1$ quasi-linear equations for $N_{el} + 1$ unknowns with bandwidth four is obtained. This numerical scheme which has a lower operation count (see Table I) than others described above, and is easier to implement, was therefore chosen for the present study.

The choice of cubic B-splines for the Galerkin approach to the solution of the KdV and MKdV equations is dictated by the requirement that the interpolation function should have a continuous second derivative throughout the solution range so that the integral formulation is possible. Similarly, a choice of quartic B-spline finite elements for the collocation method is implied by the requirement of continuity of the third derivative throughout the solution range. Higher order splines which possess higher orders of continuity could equally well be used but would result in algorithms with higher operation counts.

In Section 2 a collocation method using quartic B-spline [10, 13] finite elements is set up which shows good conservation and is both fast and accurate in performance. In validation runs the homogeneous boundary conditions described above are used, and in Section 5 forced boundary conditions are applied at one end of a finite region and the resulting states examined.

TABLE I

Methods, Finite Elements, and Operation Counts per Timestep

Method	No. eqs.	Bandwidth	$(\times/\div)$	$(+/-)$
Galerkin				
KdV	N_{el}	7	$123 \times N_{el} \times N_{it}$	$141 \times N_{el} \times N_{it}$
MKdV (cubic $f \cdot e$)	N_{el}	7	$757 \times N_{el} \times N_{it}$	$882 \times N_{el} \times N_{it}$
Collocation				
KdV (quintic $f \cdot e$)	$N_{el} + 1$	5	$36 \times N_{el} \times N_{it}$	$36 \times N_{el} \times N_{it}$
MKdV (quartic $f \cdot e$)	$N_{el} + 1$	4	$27 \times N_{el} \times N_{it}$	$32 \times N_{el} \times N_{it}$

Note. Number of elements $= N_{el}$, number of iterations $= N_{it}$.

2. FINITE ELEMENT SOLUTION

A numerical solution for the MKdV equation in the normalised form (1), over the region $0 \leqslant x \leqslant L$, is developed.

Set up $0 = x_0 < x_1 \cdots < x_N = L$ as a partition of $[0, L]$ by the points x_m into finite elements of equal size $h = (x_{m+1} - x_m)$, and let $\phi_m(x)$ be those quartic B-splines with knots at the points $x = x_m$. Then the set of splines $\{\phi_{-2}, \phi_{-1}, \ldots, \phi_N, \phi_{N+1}\}$ forms a basis for functions defined over $[0, L]$. We seek the approximation $u_N(x, t)$ to the solution $u(x, t)$ which uses these splines as trial functions [13]:

$$u_N(x, t) = \sum_{j=-2}^{N+1} \phi_j(x)\, \delta_j(t). \tag{5}$$

Each quartic B-spline covers five elements; thus each element $[x_m, x_{m+1}]$ is covered by five splines. Using a local coordinate system ζ given by $h\zeta = x - x_m$, where $0 \leqslant \zeta \leqslant 1$, expressions for the element splines are [13]

$$\begin{aligned}
\phi_{m-2} &= 1 - 4\zeta + 6\zeta^2 - 4\zeta^3 + \zeta^4 \\
\phi_{m-1} &= 11 - 12\zeta - 6\zeta^2 + 12\zeta^3 - 4\zeta^4 \\
\phi_m &= 11 + 12\zeta - 6\zeta^2 - 12\zeta^3 + 6\zeta^4 \\
\phi_{m+1} &= 1 + 4\zeta + 6\zeta^2 + 4\zeta^3 - 4\zeta^4 \\
\phi_{m+2} &= \zeta^4.
\end{aligned} \tag{6}$$

Over the element $[x_m, x_{m+1}]$ the variation of the function $u(x, t)$ is given by

$$\begin{aligned}
u(x, t) = \phi^e \cdot \mathbf{d}^e &= (\phi_{m-2}, \phi_{m-1}, \phi_m, \phi_{m+1}, \phi_{m+2}) \\
&\times (\delta_{m-2}, \delta_{m-1}, \delta_m, \delta_{m+1}, \delta_{m+2})^{\mathrm{T}}.
\end{aligned} \tag{7}$$

At the knot x_m the numerical solution $u_N(x, t)$ is given by

$$\begin{aligned}
u_m &= \delta_{m+1} + 11\delta_m + 11\delta_{m-1} + \delta_{m-2} \\
hu'_m &= 4(\delta_{m+1} + 3\delta_m - 3\delta_{m-1} - \delta_{m-2}) \\
h^2u''_m &= 12(\delta_{m+1} - \delta_m - \delta_{m-1} + \delta_{m-2}) \\
h^3u'''_m &= 24(\delta_{m+1} - 3\delta_m + 3\delta_{m-1} - \delta_{m-2}),
\end{aligned} \tag{8}$$

where the primes denote differentiation with respect to x.

We identify the collocation points with the knots, use Eqs. (8) to evaluate u_m and its space derivatives, and substitute into (1) to obtain a set of coupled ordinary differential equations, one for each knot:

$$\begin{aligned}
&\dot\delta_{m-2} + 11\dot\delta_{m-1} + 11\dot\delta_m + \dot\delta_{m+1} \\
&\quad - \frac{4\varepsilon}{h}(\delta_{m-2} + 11\delta_{m-1} + 11\delta_m + \delta_{m+1})^2 \\
&\quad \times (\delta_{m-2} + 3\delta_{m-1} - 3\delta_m - \delta_{m+1}) \\
&\quad - \frac{24}{h^3}\mu(\delta_{m-2} - 3\delta_{m-1} + 3\delta_m - \delta_{m+1}) = 0.
\end{aligned}$$

Hence with a Crank–Nicolson approximation in time, there is for each knot an equation relating parameters at adjacent time levels, δ_m^{n+1} to δ_m^n,

$$\begin{aligned}
&(1 - Z_m^{n+1/2} - M)\,\delta_{m-2}^{n+1} + (11 - 3Z_m^{n+1/2} + 3M)\,\delta_{m-1}^{n+1} \\
&\quad + (11 + 3Z_m^{n+1/2} - 3M)\,\delta_m^{n+1} \\
&\quad + (1 + Z_m^{n+1/2} + M)\,\delta_{m+1}^{n+1} \\
&= (1 + Z_m^{n+1/2} + M)\,\delta_{m-2}^{n} \\
&\quad + (11 + 3Z_m^{n+1/2} - 3M)\,\delta_{m-1}^{n} \\
&\quad + (11 - 3Z_m^{n+1/2} + 3M)\,\delta_m^{n} \\
&\quad + (1 - Z_m^{n+1/2} - M)\,\delta_{m+1}^{n}, \qquad m = 0, 1, \ldots, N
\end{aligned} \tag{9}$$

where

$$\begin{aligned}
Z_m^{n+1/2} &= \frac{2\varepsilon}{h}\Delta t(\delta_{m-2} + 11\delta_{m-1} + 11\delta_m + \delta_{m+1})^2, \\
M &= \frac{12\mu}{h^3}\Delta t, \\
\delta_m &= \frac{1}{2}(\delta_m^n + \delta_m^{n+1}).
\end{aligned} \tag{10}$$

System (9) consists of $N+1$ linear equations in $N+4$ unknowns. To obtain a unique solution to this system the three additional constraints needed are obtained from the boundary conditions:

$$\begin{aligned}
u_0, &\qquad \delta_{-2} + 11\delta_{-1} + 11\delta_0 + \delta_1 = u_0, \\
u_N = 0, &\qquad \delta_{N-2} + 11\delta_{N-1} + 11\delta_N + \delta_{N+1} = 0, \\
u'_N = 0, &\qquad \delta_{N-2} + 3\delta_{N-1} - 3\delta_N - \delta_{N+1} = 0.
\end{aligned}$$

These conditions enable us to eliminate $\delta_{-2}, \delta_N, \delta_{N+1}$ from Eq. (9) which then consists of $N+1$ linear equations in $N+1$ unknowns, $\mathbf{d} = (\delta_{-1}, \delta_0, \ldots, \delta_{N-2}, \delta_{N-1})^{\mathrm{T}}$.

The time evolution of the approximate solution $u_N(x, t)$ is determined by the time evolution of the vector $\mathbf{d}^n$. This is found by repeatedly solving the recurrence relationship (9) once the initial vector $\mathbf{d}^0$ has been computed from the initial conditions. The recurrence relationship is defective pentadiagonally so a direct algorithm for its solution exists; an inner iteration is also needed at each time step to cope with the non-linear term.

3. STABILITY ANALYSIS

A Neumann stability analysis is set up in which the growth factor of the error in a typical Fourier mode

$$\delta_j^n = \hat\delta^n e^{ijkh}, \tag{11}$$

where k is the mode number and h is the element size, is determined for the linearised scheme.

The linearisation is effected by supposing that u^2 in the non-linear term is locally constant, which is equivalent to assuming that in (10) all the δ_j^n are equal to a local constant d, so that $Z_j = Z = (2\varepsilon\,\Delta t/h)(24d)^2$ is a constant for all j and Eq. (9) is linear. Substituting the Fourier mode (11) into (9) leads to an error growth rate g of the form

$$g = \frac{a - ib}{a + ib}, \tag{12}$$

where

$$a = 2\cos\tfrac{3}{2}kh + 22\cos\tfrac{1}{2}kh,$$
$$b = 2(Z+M)\sin\tfrac{3}{2}kh + 6(Z-M)\sin\tfrac{1}{2}kh. \tag{13}$$

The modulus of $|g|$ is therefore one and the linearised scheme is unconditionally stable.

4. VALIDATION EXPERIMENT

To test the behaviour of the proposed algorithm a single soliton simulation is used. Take as initial condition Eq. (2) with $\varepsilon = 3$, $\mu = 1$, and $kp = 1.3$, $x_0 = 15$, $t = 0$. At time $t = 0$ the global trial function (5) becomes

$$u_N(x, 0) = \sum_{j=-2}^{N+1} \delta_j^0 \phi_j(x).$$

To determine the $N+4$ unknowns δ_j^0 for the validation experiment require $u_N(x, 0)$ to satisfy the following conditions;

(a) it shall agree with the initial condition $u(x, 0)$ at the knots $x_0, ..., x_N$, leading to $N+1$ conditions.

(b) its first two derivatives shall agree with those of the exact condition at x_0, i.e., $u'(x_0) = 0$ and $u''(x_N) = 0$: a further two conditions,

(c) its first derivative shall agree with that of the exact condition at x_N, i.e., $u'(x_N) = 0$: a further condition.

This leads to the matrix equation

$$\mathbf{M}\mathbf{d}^0 = \mathbf{b},$$

where

$$\mathbf{M} = \begin{bmatrix} -1 & -3 & 3 & 1 & & \\ 1 & -1 & -1 & 1 & & \\ & 1 & 11 & 11 & 1 & \\ & & \ddots & & & \\ & 1 & 11 & 11 & 1 & \\ & & 1 & 11 & 11 & 1 \\ & & -1 & -3 & 3 & 1 \end{bmatrix},$$

$$\mathbf{d}^0 = (\delta_{-2}, \delta_{-1}, \delta_0, ..., \delta_N, \delta_{N-1})^{\mathrm{T}},$$

and letting $u_j = u(x_j)$,

$$\mathbf{b} = (0, 0, u_0, u_1, ..., u_{N-1}, u_N, 0)^{\mathrm{T}}.$$

In this experiment step sizes of $\Delta t = 0.001$ and $h = 0.04$ over a range $0 \leqslant x \leqslant 40$ are used. The soliton is observed to move across the region with constant profile and velocity.

TABLE II

Single Soliton $h = 0.04$, $\Delta t = 0.001$, $0 \leqslant x \leqslant 40$

Time	$L_2 \times 10^3$	$L_\infty \times 10^3$	I_1	I_2	I_3	I_4
0.0	0.00	0.00	4.4429	3.676945	2.071337	1.050161
1.0	0.39	0.28	4.4429	3.676946	2.071338	1.050162
2.0	0.62	0.43	4.4429	3.676947	2.071337	1.050162
3.0	0.76	0.52	4.4429	3.676946	2.071338	1.050163
4.0	0.89	0.60	4.4428	3.676947	2.071336	1.050163
5.0	1.03	0.67	4.4428	3.676944	2.071336	1.050162
6.0	1.16	0.76	4.4428	3.676945	2.071338	1.050162
7.0	1.30	0.84	4.4429	3.676947	2.071338	1.050162
8.0	1.44	0.92	4.4430	3.676945	2.071338	1.050162
9.0	1.98	1.25	4.4430	3.676945	2.071337	1.050162
10.0	2.52	1.57	4.4430	3.676944	2.071337	1.050163

The error norms obtained for this validatory simulation, given in Table II, are satisfactorily small, both rising to less than $2 \times 10^{-3}\, kp$ at time $t = 10$, where kp is the amplitude of the soliton. The soliton amplitude changes from its initial value of 1.3 to 1.29972 by the end of run at $t = 10$; that is, by only $2 \times 10^{-3}\%$. The invariants, also listed in Table II, show good conservation; I_2, I_3, and I_4 remain constant to five decimal places throughout the run at $I_2 = 3.67694$, $I_3 = 2.07133$, and $I_4 = 1.05016$, changing only in the sixth decimal place, while I_1 changes from 4.4429 by only ± 1 in the fourth decimal place.

To make comparisons with published work [4], use as the initial condition Eq. (2) at $t = 0$ with $k = 1.0$, $x_0 = 15$, and $\varepsilon = 6$, $\mu = 1$ so that $p = 1.0$. Space and time steps are

TABLE III

Comparison of Single Soliton, Amplitude = 1, Simulations with Results from [4], Table I

Method	h / Δt	Time	L_∞	$\frac{I_2 - I_{20}}{I_{20}}$	$\frac{I_3 - I_{30}}{I_{30}}$
B-spline	0.1	0.25	0.0012	−0.00002	−0.00007
	0.025	0.5	0.0018	−0.00004	−0.00014
		1.0	0.0022	−0.00009	−0.00030
A-L global	0.1	0.25	0.0019	0.00009	0.00486
	0.25	0.5	0.0028	0.00017	0.00508
		1.0	0.0045	0.00033	0.00556
A-L local	0.06	0.25	0.0023	0.00002	0.00168
	0.12	0.5	0.0032	0.00003	0.00171
		1.0	0.0047	0.00006	0.00177
Implicit(*C-N*)	0.08	0.25	0.0023	0.00002	0.00297
	0.1	0.5	0.0031	0.00003	0.00298
		1.0	0.0045	0.00005	0.00303
Pseudospectral	0.625	0.25	0.0026	−0.00120	−0.02976
	0.0055	0.5	0.0041	0.00218	0.07897
		1.0	0.0046	−0.00143	−0.03534
Tappert	0.3125	0.25	0.0036	0.00000	−0.00010
	0.0041	0.5	0.0041	0.00000	−0.00013
		1.0	0.0047	0.00000	0.00001

chosen so that $L_\infty < 0.005$ at $t = 1.0$. The results are compared in Table III with others reported by Taha and Ablowitz [4] using a variety of explicit and implicit schemes, the local and global schemes proposed by Ablowitz and Ladik and the pseudospectral scheme of Fornberg and Whitham. Relative changes in the values of I_2 and I_3 are compared at various times; the values at time $t = 0$ are denoted by I_{20} and I_{30}. The present method performs well.

5. SIMULATIONS

The generation of solitary waves by boundary forcing the MKdV equation at $x = 0$ for the finite region $0 \leqslant x \leqslant x_{\max}$ is studied. Initially the region is undisturbed so that at time $t = 0$ all δ_j are zero.

The forced boundary condition applied at $x = 0$ is

$$u(0, t) = \begin{cases} U_0 \dfrac{t}{\tau}, & 0 \leqslant t \leqslant \tau, \\ U_0, & \tau < t < t_0 - \tau, \\ U_0 \dfrac{t_0 - t}{\tau}, & t_0 - \tau \leqslant t \leqslant t_0. \end{cases} \tag{14}$$

Further homogeneous boundary conditions are imposed at $x = x_{\max}$.

The effect of the impulse is to generate solitary waves at $x = 0$, which grow until they achieve a terminal amplitude, determined by the magnitude of the forced boundary value. Solitary waves are continually generated while the forcing conditions prevail; then all growth slows and eventually ceases.

5.1. *Long Impulse*

Boundary condition (14) is used with $x_{\max} = 80$, $t_{\max} = 10$, $U_0 = 1$, $\tau = 0.01$, $t_0 = 10$, so that the forcing lasts

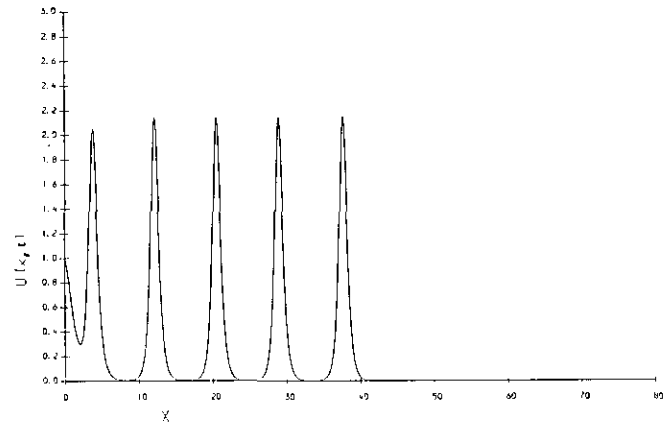

FIG. 1. *Long impulse.* Solitons produced by forced conditions (14) with $U_0 = 1$, $\tau = 0.01$, $t_0 = \infty$, $h = 0.04$, $\Delta t = 0.001$ graphed at $t = 5$ (– – –) and $t = 10$ (———); $\varepsilon = 6$.

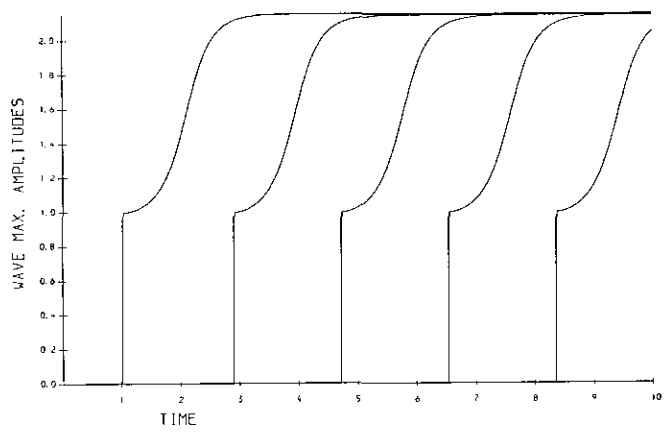

FIG. 2. *Long impulse.* The evolution of the soliton amplitudes. Forced conditions (14) with $U_0 = 1$, $\tau = 0.01$, $t_0 = \infty$, $h = 0.04$, $\Delta t = 0.001$; $\varepsilon = 6$.

throughout the experiment. The values $\varepsilon = 6$, $\mu = 1$ are taken so that $p = 1$. The step lengths are $h = 0.04$ and $\Delta t = 0.001$.

In this numerical experiment, see Fig. 1, five solitary waves are generated before the simulation is terminated at $t = 10$. Figures 2 and 3 show that four achieve their terminal heights and a constant velocity. The generating conditions for the first wave are rather more protracted than those for all subsequent waves, as can be seen from the graphs of the first two derivatives at $x = 0$ given in Figs. 4 and 5, so it achieves a slightly larger amplitude and velocity than do the following waves. The observations are collected in Table IV. The time interval between births of solitary waves is constant at $\Delta T_B = 1.82$, the measured terminal heights for solitary waves 2–4 vary between 2.147 and 2.148 with measured velocities of 4.62. Free solitons of similar heights would have velocities 4.610–4.614, so that agreement is close.

After an initial transient the graph of $u_x(0, t)$, Fig. 4,

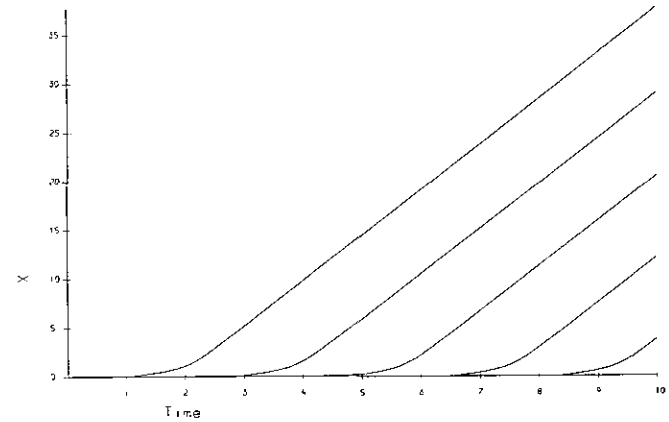

FIG. 3. *Long impulse.* The space-time graphs of the solitons produced by (14) with $U_0 = 1$, $\tau = 0.01$, $t_0 = \infty$, $h = 0.04$, $\Delta t = 0.001$; $\varepsilon = 6$.

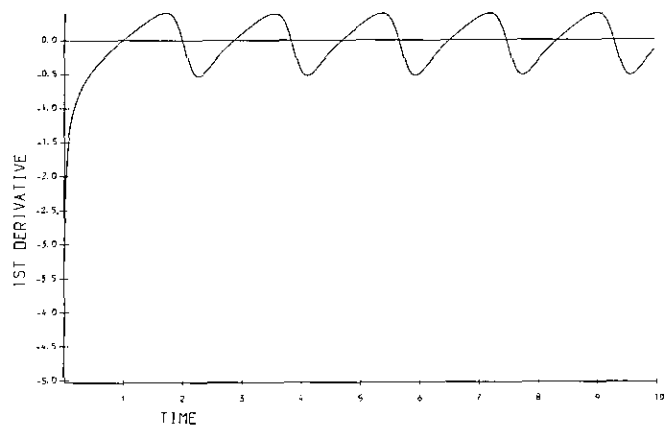

FIG. 4. *Long impulse.* Variation in the first derivative $u_x(0, t)$ at the origin. Forced conditions (14) with $U_0 = 1$, $\tau = 0.01$, $t_0 = \infty$, $h = 0.04$, $\Delta t = 0.001$; $\varepsilon = 6$.

shows a rounded saw tooth periodic behaviour with maximum of about 0.4, a minimum of about 0.33, mean zero, and period 1.82. The graph of $u_{xx}(0, t)$, Fig. 5, also exhibits periodic behaviour with period 1.82. Rewrite Eq. (1) as an expression for u_{xxx} and evaluate at $x = 0$ to give

$$u_{xxx}(0, t) = -\frac{1}{\mu}\{u_t(0, t) + \varepsilon u^2(0, t)\, u_x(0, t)\}. \quad (15)$$

With the forcing $U_0 = 1$ and $\mu = 1$, $\varepsilon = 6$, this reduces to

$$u_{xxx}(0, t) = -6u_x(0, t). \quad (16)$$

The simulation produces differentials at the origin which reflect this relationship. By comparing Figs. 2, 4, and 5 we observe that the birth of a solitary wave occurs at times when $u_x(0, t) = 0$, and $u_{xx}(0, t)$ is a minimum and negative,

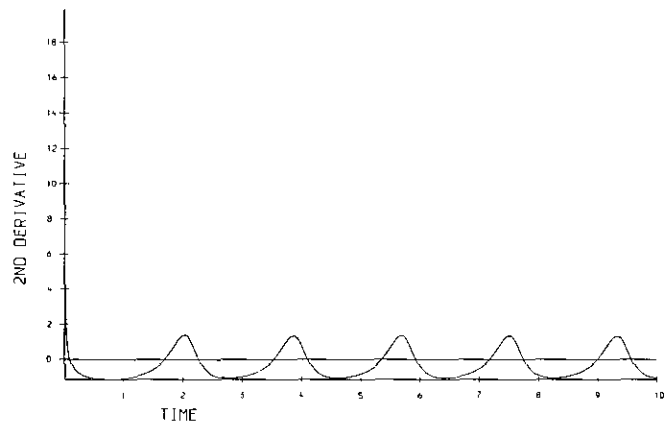

FIG. 5. *Long impulse.* Variation in the second derivative $u_{xx}(0, t)$ at the origin. Forced conditions (14) with $U_0 = 1$, $\tau = 0.01$, $t_0 = \infty$, $h = 0.04$, $\Delta t = 0.001$; $\varepsilon = 6$.

TABLE IV

Observations of Solitary Waves, $U_0 = 1$, $\varepsilon = 6$

		Generated waves		Free soliton
Wave	Birth time	Amplitude	Velocity	Velocity
1	1.040	2.155	4.64	4.644
2	2.920	2.148	4.62	4.614
3	4.740	2.147	4.62	4.610
4	6.560	2.147	4.62	4.610
5	8.380	2.058	4.27	4.235

while a solitary wave reaches maturity about $1\frac{1}{2}$ periods later when again $u_x(0, t)$ is a maximum and positive.

An experiment with reduced forcong, $U_0 = 0.5$; boundary condition (14) is used with $x_{\max} = 80$, $t_{\max} = 80$, $\tau = 0.01$, $t_0 = 80$. The forcing lasts throughout the experiment. The numerical step lengths are $h = 0.04$ and $\Delta t = 0.001$. Observations on the solitary waves generated are collected in Table V. The period between births is $\Delta T_B = 14.632$.

An experiment with increased forcing, $U_0 = 2$; boundary condition (14)' is used with $x_{\max} = 24$, $t_{\max} = 1.5$, $\tau = 0.1$, $t_0 = 1.5$. The forcing again lasts throughout the experiment. The numerical step lengths are $h = 0.01$ and $\Delta t = 0.0005$. It is observed that solitary waves are generated with period $\Delta T_B = 0.2271$, and, apart from the initial wave, all subsequent waves attain a terminal height of 4.295 with velocity 18.25, which compares well with the free soliton velocity of 18.28.

5.2. *Short Impulse*

In this simulation boundary condition (14) is used with $U_0 = 1$, $\tau = 0.01$, $t_0 = 4$, $h = 0.04$, and $\Delta t = 0.001$. The values $\varepsilon = 3$, $\mu = 1$ are taken so that $p = 1.4142$. Two solitary waves are generated in the experiment, of which only the first, born at $t = 2.84$, reaches its mature amplitude 2.15 and velocity 2.31; the second, born at $t = 8.14$, grows to an amplitude 1.43 with a velocity 1.02.

The invariants I_j, (Eq. (3)), are only constant when the

TABLE V

Observations of Solitary Waves, $U_0 = 0.5$, $\varepsilon = 6$

		Generated waves		Free soliton
Wave	Birth time	Amplitude	Velocity	Velocity
1	8.08	1.0783	1.164	1.163
2	23.119	1.0749	1.155	1.155
3	37.751	1.0743	1.152	1.154
4	52.303	1.0745	1.152	1.155
5	66.815	0.5014		0.251

boundary conditions $u \to 0$ as $x \to \pm\infty$ hold. With the forcing conditions (14) it is found that they vary in the following ways:

$$I_1(t) = I_1(0) + \int_0^t \left\{ \frac{1}{3}\varepsilon u^3(0, t) + \mu u_{xx}(0, t) \right\} dt$$

$$I_2(t) = I_2(0) + \int_0^t \left\{ \frac{1}{4}\varepsilon u^4(0, t) + \mu u(0, t)\, u_{xx}(0, t) - \frac{1}{2}\mu u_x^2(0, t) \right\} dt$$

$$I_3(t) = I_3(0) + \int_0^t \left\{ \frac{2}{3}\varepsilon u^6(0, t) + 4\mu u^3(0, t)\, u_{xx}(0, t) + 6\frac{\mu^2}{\varepsilon} u_{xx}^2(0, t) - 12\frac{\mu}{\varepsilon} u_x(0, t)\, u_t(0, t) \right\} dt$$

$$I_4(t) = I_4(0) + \int_0^t \left\{ -\frac{3}{4}\varepsilon u^8(0, t) + \mu\{45u^4(0, t)\, u_x^2(0, t) - 6u^5(0, t)\, u_{xx}(0, t)\} + 3\frac{\mu^2}{\varepsilon}\{20u^2(0, t)\, u_x(0, t)\, u_{xxx}(0, t) - 16u^2(0, t)\, u_{xx}^2(0, t) - u_x^4(0, t) - 20u(0, t)\, u_x^2(0, t)\, u_{xx}(0, t)\} + 36\frac{\mu^3}{\varepsilon^2}\left\{ \frac{1}{2}u_{xxx}^2(0, t) - u_{xx}(0, t)\, u_{xxxx}(0, t) \right\} \right\} dt.$$

Using (15) it can be shown that the variation of the I_j depends only on the behaviour of $u(0, t)$, $u_x(0, t)$, and $u_{xx}(0, t)$. Hence over the time period $0 \leqslant t \leqslant 11$, with $\varepsilon = 3$, $\mu = 1$, and $0(0, t) = 1$ the variation in quantities I_j is given by

$$I_1(t) = \int_0^t \{1 + u_{xx}(0, t)\}\, dt$$

$$I_2(t) = \int_0^t \{\tfrac{3}{4} + u_{xx}(0, t) - \tfrac{1}{2}u_x^2(0, t)\}\, dt$$

$$I_3(t) = \int_0^t \{2 + 4u_{xx}(0, t) + 2u_{xx}^2(0, t)\}\, dt$$

$$I_4(t) = \int_0^t \{-\tfrac{9}{4} + 3u_x^2(0, t) - 4u_{xx}^2(0, t) - 6u_{xx}(0, t) - u_x^4(0, t) + 4u_x^2(0, t)\, u_{xx}(0, t) + 4u_{xx}(0, t)\, u_{xt}(0, t)\}\, dt,$$

so that all change continuously, although the rates will vary since all three integrands vary periodically as is illustrated by the graphs of $u_x(0, t)$ and $u_{xx}(0, t)$ given in Figs. 4 and 5.

TABLE VI

Invariants for Forced Conditions with $t_0 = 11$, $U_0 = 1$

Time	I_1	I_2	I_3	I_4
0	0.0000	0.0000	0.0000	0.0000
3	2.1478	1.4277	0.4819	79.110
6	5.0569	5.6259	7.2503	357.44
9	7.0409	7.9485	10.380	1498.8
12	8.7486	10.175	12.222	1918.6
15	8.8961	10.156	12.244	1888.6
18	8.9055	10.156	12.244	1891.6
21	8.9043	10.156	12.244	1892.8
24	8.9026	10.156	12.244	1893.3
27	8.9011	10.156	12.244	1893.3
30	8.8999	10.156	12.244	1893.3

When the forcing is turned off at $t = 11$, for $t > 11$, $u(0, t) = 0$; but as the derivatives $u_x(0, t)$ and $u_{xx}(0, t)$ are not themselves forced to become zero, the I_j do not immediately cease to vary. In the simulations the switching operation causes a spike in the derivative graphs, and subsequently $u_{xx}(0, t)$ and $u_x(0, t)$ tend to zero at about the same rate. Thus I_1 continues to change, increasing or decreasing according to the sign of $u_{xx}(0, t)$, through

$$I_1(t) = I_1(11) + \int_{11}^t u_{xx}(0, t)\, dt;$$

I_2 starts to decrease through

$$I_2(t) = I_2(11) - \int_{11}^t \tfrac{1}{2}u_x^2(0, t)\, dt;$$

and I_3 to increase through

$$I_3(t) = I_3(11) + 2\int_{11}^t u_{xx}^2(0, t)\, dt;$$

and I_4 changes through

$$I_4(t) = I_4(11) - \int_{11}^t \{u_x^4(0, t) - 4u_{xx}(0, t)\, u_{xt}(0, t)\}\, dt.$$

TABLE VII

Mean Observations of Solitary Waves: Long Impulse, Various Forcing

ε	p	U_0	ΔT_B	Amplitude	Velocity
6	1.0	0.5	14.552	1.0746	1.153
6	1.0	1.0	1.82	2.147	4.62
6	1.0	2.0	0.2271	4.295	18.25
3	1.4142	0.5	41.25	1.073	0.572
3	1.4142	1.0	5.15	2.147	2.31

These equations also imply that the development of the last formed solitary wave does not stop abruptly when the forcing is switched off, but that it continues until $u_x(0, t)$ and $u_{xx}(0, t)$ have decayed to zero. After a time of about $t = 15$, when the influences of forcing have died away, the quantities I_j should remain constant. The above conclusions are illustrated by the measured values of the invariants given in Table VI.

6. DISCUSSION

The numerical solution algorithm for the MKdV equation, based on collocation of quartic B-splines over finite elements, described in Section 2, is validated in Section 4 by a single soliton simulation, which shows good conservation and accuracy.

The simulation reported in Section 5 show that constant positive boundary forcing produces a train of solitary waves of like amplitude and velocity generated at a constant rate. The initial wave has a slightly larger amplitude due to a switch-on effect. This behaviour is qualitatively similar to that of the KdV equation under identical conditions [5, 6, 11].

Characteristic results for the numerical experiments on positive boundary forcing for various parameter values are listed in Table VII. It is deduced that solitary waves are generated with period $\Delta T_B = 1.82(p/U_0)^3$, amplitude $2.147 \times U_0$, and velocity $4.62 \times U_0^2$, where U_0 is the magnitude of the forcing; the definition of p follows Eq. (2).

The birth times recorded in Tables IV and V and referred to in the text are those at which a solitary wave *starts* to traverse the region. Some short time before this the solitary wave is conceived at the origin as a localised disturbance which begins to develop. If the forcing is removed before separation from the origin (birth) occurs the solitary wave never forms and the small local disturbance which remains located near the origin dies away as the simulation proceeds.

In further simulations it has been shown that negative forcing, $-U_0$, produces negative solitary waves of equal amplitude to those produced by positive forcing, U_0. The final state, produced when a positive impulse is followed by an equal negative impulse, depends on the periodicity of the forcing as well as its magnitude.

The solitary waves generated by boundary forcing have amplitudes and velocities consistent with those of the free soliton solution of the MKdV equation and when they interact they behave similarly and show the expected phase shifts ϑ, Eq. (3). Although these observations are subject to experimental error they tend to support the idea that these solitary waves are indeed identical with free solitons.

It has been shown that the collocation method with quartic B-spline finite elements can faithfully represent the amplitude, position, and velocity of a single soliton and that the generation of solitons by boundary forcing is modelled satisfactorily.

ACKNOWLEDGMENT

T. G. wishes to thank the University of Inonu, Republic of Turkey, for the award of a research scholarship and for financial support during the course of this work.

REFERENCES

1. N. J. Zabusky and M. D. Kruskal, *Phys. Rev. Lett.* **15**, 240 (1965).
2. A. Jeffrey and T. Kakutani, *SIAM Rev.* **14**, 582 (1972).
3. B. Fornberg and G. B. Whitham, *Philos. Trans. R. Soc.* **289**, 373 (1978).
4. T. R. Taha and M. J. Ablowitz, *J. Comput. Phys.* **77**, 540 (1988).
5. C. K. Chu, L. W. Xiang, and X. Baransky, *Commun. Pure Appl. Math.* **36**, 495 (1983).
6. R. Camassa and T. Y. Wu, *Wave Motion* **11**, 495 (1989).
7. Q. Chang and B. Guo, *J. Comput. Phys.* **93**, 360 (1991).
8. G. A. Gardner, L. R. T. Gardner, and A. H. A. Ali, in *Numerical Methods in Engineering*, edited by G. N. Pande and J. Middleton (Elsevier Applied Science, London, 1990), Vol. 1, p. 590.
9. L. R. T. Gardner and G. A. Gardner, *J. Comput. Phys.* **101**, 218 (1992).
10. G. A. Gardner, L. R. T. Gardner, and A. H. A. Ali, in *Mathematics Numerical Aspects of Wave Propagation*, edited by G. Cohen *et al.* (SIAM, Philadelphia, 1991), p. 533.
11. L. R. T. Gardner, G. A. Gardner, and I. Dag, *Int. J. Numer. Methods Eng.* **36**, 3317 (1993).
12. L. R. T. Gardner, G. A. Gardner, and A. H. A. Ali, in *Proceedings, Fifth Inter Symp. Numer. Methods in Eng.*, edited by R. Gruber, J. Periaux, and R. P. Shaw (Springer-Verlag, Berlin, 1989), Vol. 2, p. 565.
13. P. M. Prenter, *Splines and Variational Methods* (Wiley, New York, 1975).